Monthly Notices
of the
ROYAL ASTRONOMICAL SOCIETY

Mon. Not. R. Astron. Soc. **427,** 1517–1529 (2012) doi:10.1111/j.1365-2966.2012.21837.x

The light-curve modulation of XY And and UZ Vir: two Blazhko RR Lyrae stars with additional frequencies⋆

Á. Sódor,[1]† G. Hajdu,[1] J. Jurcsik,[1] B. Szeidl,[1] K. Posztobányi,[2] Zs. Hurta,[2] B. Belucz[3] and E. Kun[4]

[1]*Konkoly Observatory, Research Centre for Astronomy and Earth Sciences, Hungarian Academy of Sciences, Budapest, Hungary*
[2]*Visiting astronomer at Konkoly Observatory*
[3]*Eötvös University, Department of Astronomy, PO Box 49, H-1518 Budapest, Hungary*
[4]*Department of Experimental Physics and Astronomical Observatory, University of Szeged, 6720 Szeged, Dóm tér 9, Hungary*

Accepted 2012 July 31. Received 2012 July 27; in original form 2012 June 15

ABSTRACT

We present a thorough analysis of multicolour CCD observations of two modulated RRab-type variables, XY And and UZ Vir. These Blazhko stars show relatively simple light-curve modulation with the usual multiplet structures in their Fourier spectra. One additional, independent frequency with linear-combination terms of the pulsation frequency is also detected in the residual spectrum of each of the two stars. The amplitude and phase relations of the triplet components are studied in detail. Most of the epoch-independent phase differences show a slight, systematic colour dependence. However, these trends have opposite signs in the two stars. The mean values of the global physical parameters and their changes with the Blazhko phase are determined, utilizing the inverse photometric method (IPM). The modulation properties and the IPM results are compared for the two variables. The pulsation period of XY And is the shortest when its pulsation amplitude is the highest, while UZ Vir has the longest pulsation period at this phase of the modulation. Despite this contrasting behaviour, the phase relations of the variations in their mean physical parameters are similar. These results do not agree with the predictions of the Blazhko model of Stothers.

Key words: techniques: photometric – stars: horizontal branch – stars: individual: XY And – stars: individual: UZ Vir – stars: oscillations – stars: variables: RR Lyrae.

1 INTRODUCTION

Although research activity in this field has recently increased, we still do not have a satisfactory model for the phenomenon of the light-curve modulation of RR Lyrae stars, the so-called Blazhko effect, which would be consistent with the wide variety of the ever-increasing collection of observations. To find such a model, we need not only to know the phenomenology of the light-curve variation. The modulational changes in the atmospheric physical parameters of these stars also impose constraints on potential Blazhko models. The brightness variations of Blazhko RR Lyrae stars can be studied with unprecedented detail and precision using the data of the *Convection rotation and planetary transits* (*CoRoT*) and *Kepler* space telescopes in a single photometric band. These studies have led to new explanations of the phenomenon with the detection of half-integer frequencies (Kolláth, Molnár & Szabó 2011; Buchler & Kolláth 2012). However, standard multicolour or spectroscopic observations are needed to derive physical parameters. Because the modulation periods of Blazhko stars span a wide range, from about one week to many hundreds of days, detailed spectroscopic studies using telescopes with sufficiently large apertures are difficult to attain. Therefore, moderate-sized Earth-based multicolour photometric telescopes still have an important role in the study of the Blazhko effect.

In the context of the Konkoly Blazhko Surveys I and II (Jurcsik et al. 2009; Sódor et al. 2012), we have obtained multicolour light curves of bright, northern, fundamental-mode Blazhko RR Lyrae stars. These data have already been successfully utilized to derive the variations in the atmospheric parameters of six modulated stars (see section 6 in Jurcsik et al. 2012, and references therein).

According to the explanation of Stothers (2006), the Blazhko effect is 'a direct consequence of a gradual strengthening and weakening of turbulent convection in the stellar envelope'. Although this model has been seriously criticized on theoretical grounds by

⋆Based on observations collected with the automatic 60-cm telescope of Konkoly Observatory, Svábhegy, Budapest.
†E-mail: sodor@konkoly.hu

Table 1. Log of the CCD observations of XY And and UZ Vir obtained with the 60-cm automatic telescope of the Konkoly Observatory.

Object	From (JD − 245 0000)	To	Filter	Nights	Data points
XY And	4390	4857	V	64	2611
			I_C	64	2610
UZ Vir	4504	4978	B	72	1722
			V	70	1695
			I_C	70	1676

Table 2. Identification of the variables and their comparison stars.

Object	2MASS ID	Comp. star 2MASS ID
XY And	01264243+3404068	01270016+3404307
UZ Vir	13084432+1324084	13082756+1322403

Kovács (2009), Smolec et al. (2011) and Molnár, Kolláth & Szabó (2012), it is important to test the predictions of the Stothers model with observational results. The model predicts that the phase relation between the amplitude and period changes depends on the mean physical properties of the star, and that this is also directly connected with the phase relations of the physical parameter variations during the Blazhko cycle. In this present paper, we aim to test whether there is any connection between the phase relation of the amplitude and period (phase) variations and the mean physical parameters and their variations during the Blazhko cycle, as proposed by Stothers (2006, 2011). Therefore, in order to study their Blazhko modulation in detail, we have selected two stars, XY And ($\alpha_{2000} = 01^{\rm h}26^{\rm m}42\overset{\rm s}{.}43$, $\delta_{2000} = +34^\circ04'06\overset{''}{.}9$, $P = 0.3987$ d, $P_{\rm mod} = 41.4$ d) and UZ Vir ($\alpha_{2000} = 13^{\rm h}08^{\rm m}44\overset{\rm s}{.}32$, $\delta_{2000} = +13^\circ24'08\overset{''}{.}4$, $P = 0.4593$ d, $P_{\rm mod} = 68.2$ d). These two stars show different phase relations between their amplitude and period (phase) variations. XY And and UZ Vir were extensively observed in the course of the Konkoly Blazhko Survey I (Jurcsik et al. 2009), but the data and the results of the light-curve analysis have not yet been published.

2 OBSERVATIONS

Multicolour CCD observations of XY And and UZ Vir were obtained between 2008 February and 2009 May, and between 2007 October and 2009 January, respectively, with the 60-cm automatic telescope of Konkoly Observatory at Svábhegy, Budapest, equipped with a 750 × 1100 Wright Instruments CCD camera. In the case of UZ Vir, Johnson–Cousins BVI_C filters were used. For XY And, which is ∼0.7 mag fainter, the observations were carried out only in the V and I_C bands, in order to ensure a reasonably short duty cycle. In each band, the total numbers of the observations are about 2600 and 1700 for XY And and UZ Vir, respectively (see Table 1 for the log of observations). Standard CCD calibration and aperture photometry were performed on all the object frames using IRAF[1] packages. The relative magnitudes of the variables were measured against the nearby comparison stars identified in Table 2, and they were transformed to the Johnson–Cousins system using standard procedures.

[1] IRAF is distributed by the National Optical Astronomy Observatories, which are operated by the Association of Universities for Research in Astronomy, Inc., under cooperative agreement with the National Science Foundation.

Fig. 1 shows the light curves of the variables folded with the pulsation period at selected Blazhko phases.

The light-curve data of XY And and UZ Vir are available as Supporting Information with the online version of this paper. Tables A1–A5 in Appendix A give information regarding the form and content of the data.

3 FREQUENCY ANALYSIS

A mathematical description of the light curves is sought by discrete Fourier transform (Deeming 1975), as implemented in the MUFRAN package (Kolláth 1990), the GNUPLOT utilities[2] and a non-linear fitting algorithm (Sódor 2012).

A peak in the Fourier spectrum is accepted as an independent frequency of the star and is included in the solution if its amplitude exceeds 3.5σ in at least two photometric bands (σ is defined as the local mean level of the residual spectrum). For linear-combination terms of the independent frequencies, the selection criterion is that its amplitude exceeds 2.5σ in at least two bands, or 3σ in one band.

3.1 Pulsation and modulation components

The top panels of Fig. 2 show the spectra of the V light curves of XY And and UZ Vir. The bottom panels display the residual spectra after pre-whitening for the pulsation frequency and its harmonics (kf_0). The window functions are plotted in the insets. Sidepeaks belonging to the modulation triplet frequencies ($kf_0 \pm f_{\rm m}$), with significantly different amplitudes of the two components, are clearly identified in the residual spectrum of the variables. After pre-whitening for the pulsation frequency, its harmonics, the modulation frequency and their identified linear-combination terms, no further triplet (multiplet) structure, which can indicate a secondary modulation, is found around the pulsation frequency and its harmonics in any of the stars.

3.2 Detection of additional frequencies

Fig. 3 shows the residual spectra of XY And and UZ Vir in the observed bands after the removal of the detected multiplets. Both spectra have a regular pattern of peaks with separations of the pulsation frequency, f_0. The frequency values, the f_0/f frequency ratios, the amplitudes and their significance are given in Table 3. Most probably, one of these frequencies is an additional (radial or non-radial) mode, while the other peaks are linear combinations of this mode and the pulsation frequency. For UZ Vir, ± 1 c d^{-1} alias solutions for the identification of the 'base' frequency of the additional frequency series cannot be excluded either.

3.2.1 Additional frequency of XY And

We accept the second of the series listed in Table 3 ($f_2' = 7.7202$) as an independent, additional frequency, because it has the highest amplitude, in both the V and I_C bands. This frequency can be identified as a non-radial mode, because model calculations (Buchler & Kolláth 2001; Kolláth et al. 2011) indicate that neither normal nor 'strange' modes have positive growth rates with a frequency ratio around 0.325, which is between the regime of the fifth and sixth radial overtones (see fig. 3 in Kolláth et al. 2011).

[2] http://www.gnuplot.info/

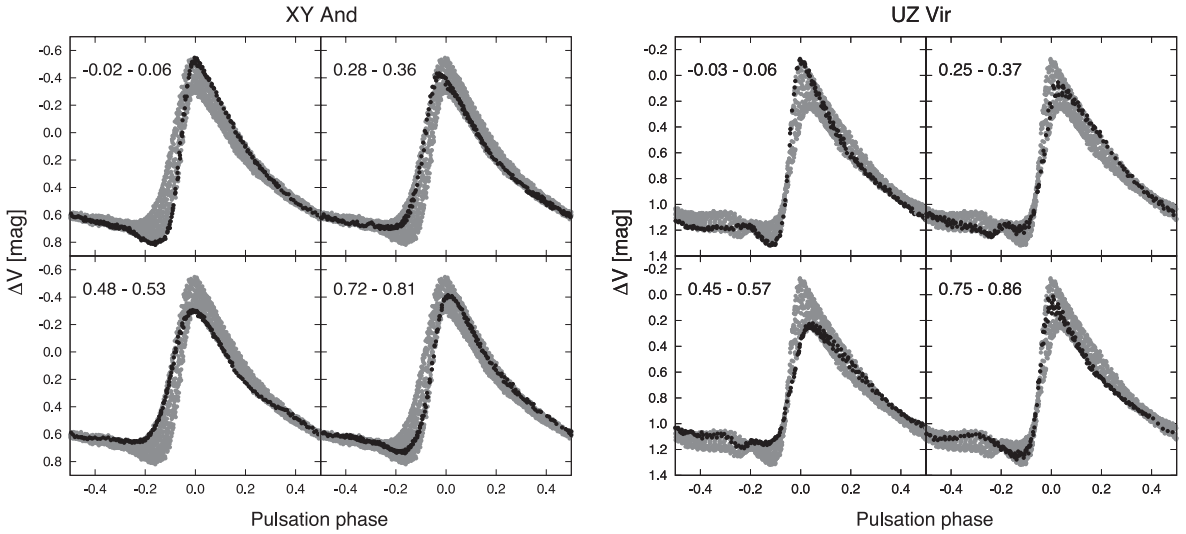

Figure 1. Folded *V* light curves of XY And and UZ Vir in selected Blazhko phase bins. The grey dots indicate all the measurements. In the top-left corners, the Blazhko-phase ranges of the highlighted data are given, according to the Blazhko ephemerides (equations 2 and 4). The rising branch of XY And shows a significant phase variation (∼0.1 pulsation phase) while the fix point on the rising branch of UZ Vir indicates that amplitude modulation dominates its light-curve variation. The phase of the maximum brightness varies, however, within about the same ±0.02 pulsation-phase range in both stars, as shown in Fig. 4.

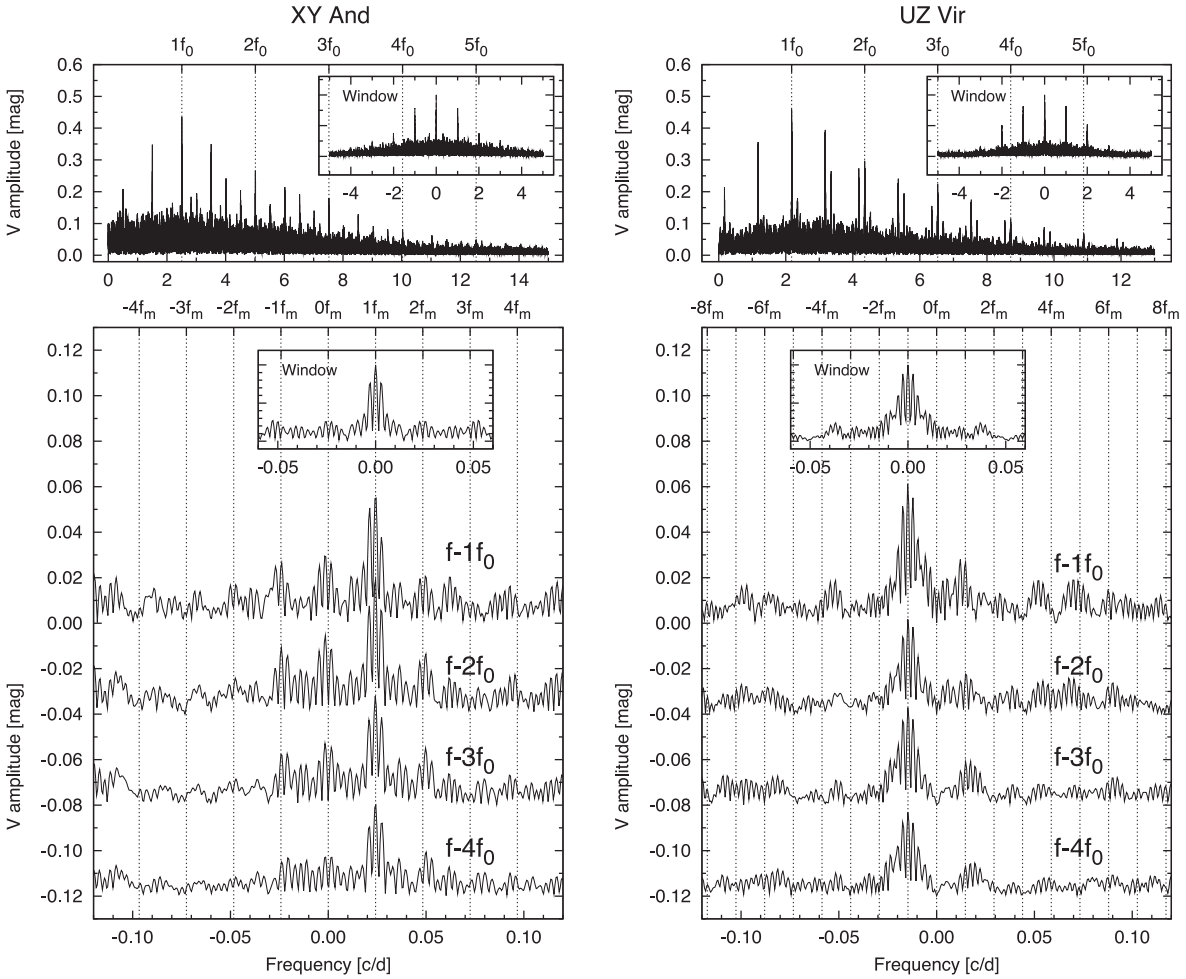

Figure 2. Fourier amplitude spectra of the *V* light curves of XY And and UZ Vir (top panels). The residual spectra are plotted in the bottom panels around the first four harmonics of the pulsation frequency after the removal of the detected pulsation components (kf_0, $k = \{1, \ldots, 13\}$ for XY And and $k = \{1, \ldots, 25\}$ for UZ Vir). The spectrum segments are artificially shifted for clarity. Peaks belonging to the modulation ($kf_0 \pm f_m$) are clearly identified. The window functions, shown in the insets, demonstrate that no high-amplitude alias frequencies are present besides the daily and yearly aliases.

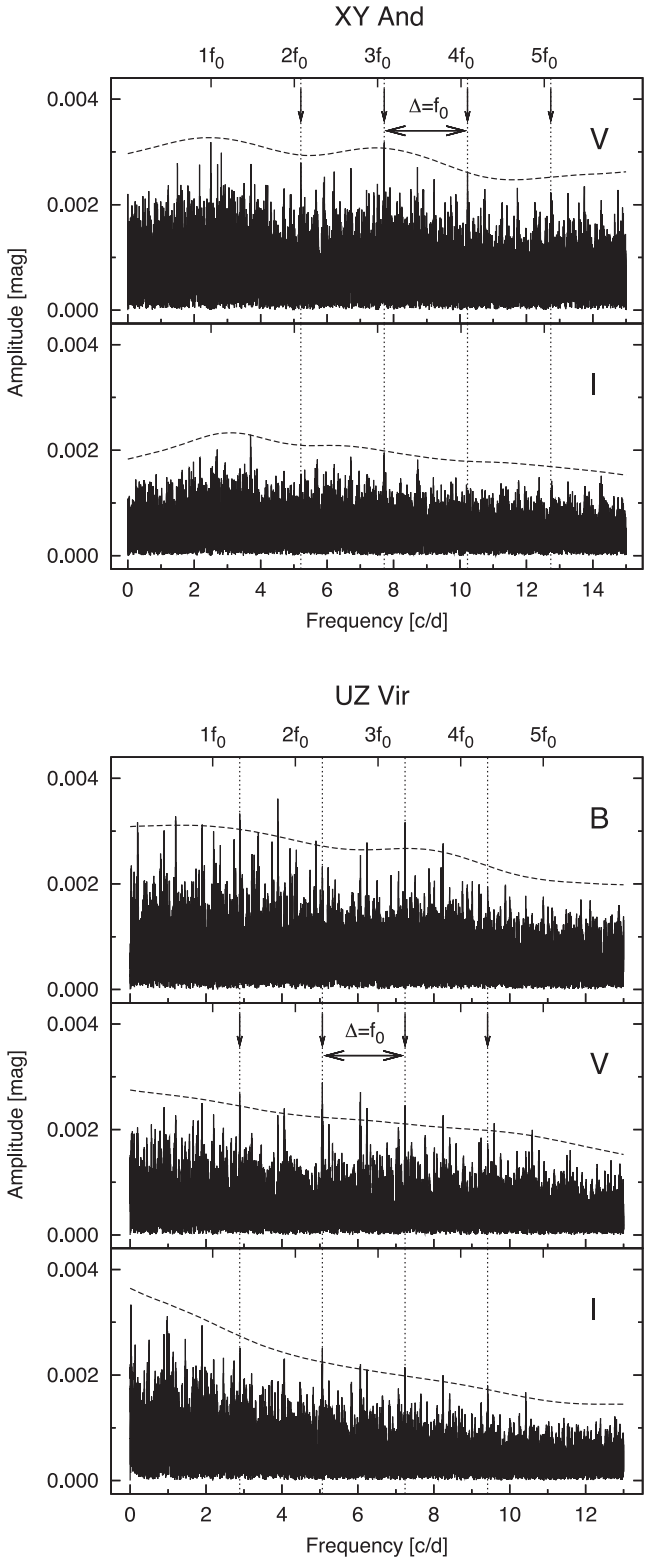

Figure 3. Residual amplitude spectra of XY And and UZ Vir in the observed bands after the removal of the pulsation frequency, its harmonics, the modulation frequency and their linear combinations. Dashed lines show 3.5 times the mean level of the spectra (3.5σ). A regular pattern is evident in the spectra of both stars: peaks are present at 5.21, 7.72, 10.23 and 12.74 c d^{-1} and at 2.89, 5.06, 7.24 and 9.42 c d^{-1} in the case of XY And and UZ Vir, respectively. These frequency series (indicated by vertical dotted lines) are separated by the pulsation frequency.

Table 3. The sequences of identified additional frequencies in XY And and UZ Vir. The ratios with the pulsation frequency (f_0/f_i'), the amplitudes and the significance are given. For UZ Vir, the ±1 c d^{-1} alias frequencies are also listed.

	Freq. (c d^{-1})	f_0/f_i'	$A(B)$ (mag)	σ	$A(V)$ (mag)	σ	$A(I)$ (mag)	σ
			XY And					
f_1'	5.2122	0.481	–	–	0.0028	3.3	0.0013	2.2
f_2'	7.7202	0.325	–	–	0.0032	3.6	0.0019	3.5
f_3'	10.2282	0.245	–	–	0.0026	3.5	0.0011	2.2
f_4'	12.7362	0.197	–	–	0.0022	3.1	0.0011	2.3
			UZ Vir					
f_1'	2.8880	0.754	0.0033	3.8	0.0027	3.9	0.0019	2.4
f_2'	5.0648	0.430	0.0023	3.0	0.0029	4.5	0.0025	3.9
f_3'	7.2416	0.301	0.0032	4.2	0.0025	4.2	0.0021	3.7
f_4'	9.4184	0.231	0.0019	2.8	0.0017	3.0	0.0018	3.7
$f_1'^-$	1.8880	1.153	0.0032	3.9	0.0022	3.3	0.0015	2.1
$f_2'^-$	4.0648	0.536	0.0021	2.8	0.0025	4.0	0.0022	3.6
$f_3'^-$	6.2416	0.349	0.0027	3.6	0.0021	3.6	0.0020	3.7
$f_4'^-$	8.4184	0.259	0.0018	3.0	0.0016	2.9	0.0017	3.8
$f_1'^+$	3.8880	0.560	0.0022	2.5	0.0021	2.9	0.0018	2.0
$f_2'^+$	6.0648	0.359	0.0018	2.2	0.0022	3.3	0.0023	3.3
$f_3'^+$	8.2416	0.264	0.0023	3.0	0.0019	3.1	0.0016	2.7
$f_4'^+$	10.4184	0.209	0.0017	2.3	0.0017	2.9	0.0013	2.5

The explanation that these peaks belong to a secondary modulation series, with ∼0.196 c d^{-1} separation from the harmonics of the pulsation, cannot be excluded either. However, both the corresponding extremely short modulation period (∼5.01 d) and the lack of the triplet components on the other side of the pulsation frequency make this explanation less likely.

3.2.2 *Additional frequency of UZ Vir*

In the case of UZ Vir, any of the f_1', f_2' and f_3' frequencies can be considered as the base frequency of the additional frequency series; f_1' and f_3' are strong in the B band, while the amplitude of f_2' is highest in the V and I_C bands. When fitting the final frequency solution to the light curves, f_2' was treated as a mathematically independent frequency, but this technical choice does not affect our subsequent results and conclusions.

As Fig. 3 shows, the ±1 c d^{-1} alias frequencies of the additional frequency series of UZ Vir have similar amplitudes as those selected, which poses further ambiguities. Fitting the light curve of UZ Vir with all the detected frequencies and with the series of f_i' listed in the first block of Table 3, the rms values of the residuals are 0.0112, 0.0093 and 0.0096 mag in the B, V and I_C bands, respectively. The solutions including the $f_i'^+$ and $f_i'^-$ alias frequency series yield marginally higher rms values of the residuals: 0.0113, 0.0095, 0.0097 and 0.0114, 0.0094, 0.0097 mag, respectively. Moreover, all amplitudes of the f_1', f_2', f_3' and f_4' terms in the B, V and I_C bands are higher than the corresponding amplitudes of the possible alias solutions. These results support our choice of the true additional frequency series of UZ Vir.

The frequency at 2.888 c d^{-1} (f_1') has a period ratio of 0.754 with f_0. Although this is significantly larger than the observed f_0/f_1

Table 4. Pulsation, modulation and additional frequencies, the corresponding periods and their errors (in parentheses, in the unit of the last digit) of XY And and UZ Vir.

	Frequency (c d^{-1})	Period (d)
	XY And	
Pulsation (f_0, P_0)	2.5079961(6)	0.3987247(1)
Modulation (f_m, P_m)	0.02417(3)	41.37(5)
Additional (f_2', P_2')	7.7202(6)	0.12953(1)
	UZ Vir	
Pulsation (f_0, P_0)	2.1767879(4)	0.4593925(1)
Modulation (f_m, P_m)	0.014654(3)	68.24(1)
Additional (f_2', P_2')	5.06481(6)	0.197441(2)

period ratios of double-mode RR Lyrae stars, an open question is whether, in special, resonant cases, a low-amplitude, first-overtone mode might really be excited at such a large frequency ratio (Z. Kolláth, private communication). The frequency of the other possible base component of this additional frequency series ($f_2' = 5.065$ or $f_3' = 7.242$) might be identified as the third/fourth and the sixth-order radial mode or a non-radial mode. However, because RR Lyrae models show that radial modes between the third and eighth radial orders are strongly damped, this explanation seems to be unlikely. It is important to note here that, according to the study of Dziembowski & Cassisi (1999), non-radial modes also have the highest chances for excitation at close proximity to the radial modes. The explanation of the additional frequency series as a secondary modulation is rejected in this case, because the peaks are at a distance of 0.711 c d^{-1} from the pulsation harmonics, which corresponds to an unlikely short modulation period of only ∼1.41 d.

3.3 Final frequency solution

None of the residual spectra shows any further significant peak after the removal of the frequency components identified in the previous subsections. No frequency component with an amplitude larger than 3.5σ in at least one band is detected within the 0.05 d^{-1} vicinity of the positions of the half-integer pulsation frequencies ($kf_0/2$, $k = 1$, 3, 5, 7, 9) in either of the two stars.

The final frequency solution of XY And includes 57 components: 13 harmonics of the pulsation frequency (kf_0), the modulation frequency (f_m), 24 linear-combination frequencies belonging to the triplets ($kf_0 \pm f_m$), 15 quintuplet components ($kf_0 \pm 2f_m$), the additional frequency (f_2' in Table 3) and three linear combinations of the additional frequency and the pulsation frequency. The rms values of the residuals are 0.011 and 0.008 mag in the V and I_C bands, respectively.

As for UZ Vir, the total number of identified frequency components is 84. Of these, 25 are harmonics of the pulsation frequency, one is the modulation frequency, 42 are triplet components, 11 are quintuplet components, one is a septuplet peak ($6f_0 - 3f_m$), another is the additional frequency and three linear combinations of the additional frequency and the pulsation frequency are also included. The rms values of the residuals are 0.011, 0.009 and 0.010 mag in the B, V and I_C bands, respectively.

The accepted values of the independent frequencies (f_0, f_m, f_2') are determined by a non-linear Fourier fit to the V light curves of the stars, including all the identified linear-combination components with locked frequencies. These frequency values, the corresponding periods and their errors are listed in Table 4. The tables containing the full light-curve solutions (the frequency components, amplitudes and phases in each band) are available as Supporting Information with the online version of this paper. Tables 5 and 6 are samples of

Table 5. Frequencies, amplitudes and phases of the V and I_C light-curve solutions (epoch =54390.0, sine decomposition) of XY And. The full table is available as Supporting Information with the online version of this paper.

	XY And				
		V		I_C	
Identification	f (c d^{-1})	Amplitude (mag)	Phase (rad)	Amplitude (mag)	Phase (rad)
f_0	2.507996	0.4263(3)	5.275(1)	0.2574(3)	5.139(1)
$2f_0$	5.015992	0.2044(3)	0.275(2)	0.1267(3)	0.241(2)
...					
f_m	0.024171	0.0101(3)	3.11(3)	0.0062(3)	3.34(4)
$f_0 + f_m$	2.532167	0.0528(3)	6.107(6)	0.0320(3)	6.127(8)
$2f_0 + f_m$	5.040163	0.0506(3)	1.190(7)	0.0317(3)	1.278(8)
...					
$f_0 - f_m$	2.483825	0.0225(3)	2.07(2)	0.0138(3)	2.19(2)
$2f_0 - f_m$	4.991821	0.0239(3)	3.47(1)	0.0150(3)	3.53(2)
...					
$3f_0 + 2f_m$	7.572330	0.0018(3)	2.9(2)	0.0016(3)	3.0()
$4f_0 + 2f_m$	10.08033	0.0016(3)	4.9(2)	0.0009(3)	5.6(3)
...					
$f_0 - 2f_m$	2.459654	0.0030(3)	5.5(1)	0.0019(3)	5.8(1)
$2f_0 - 2f_m$	4.967650	0.0015(4)	5.9(2)	0.0010(3)	5.2(3)
...					
$f_1' = f_2' - f_0$	5.212223	0.0026(4)	5.5(1)	0.0012(3)	0.1(2)
f_2'	7.720219	0.0029(4)	0.4(1)	0.0019(3)	0.8(2)
$f_3' = f_2' + f_0$	10.22822	0.0021(4)	2.7(2)	0.0006(3)	2.2(5)
$f_4' = f_2' + 2f_0$	12.73621	0.0017(4)	4.0(2)	0.0009(3)	4.2(3)

Table 6. Frequencies, amplitudes and phases of the B, V and I_C light-curve solutions (epoch = 54404.0, sine decomposition) of UZ Vir. The full table is available as Supporting Information with the online version of this paper.

UZ Vir							
		B		V		I_C	
Identification	f (c d^{-1})	Amplitude (mag)	Phase (rad)	Amplitude (mag)	Phase (rad)	Amplitude (mag)	Phase (rad)
f_0	2.176788	0.5485(4)	0.867(1)	0.4193(4)	0.826(1)	0.2603(4)	0.681(1)
$2f_0$	4.353576	0.2531(4)	3.930(2)	0.1993(3)	3.936(2)	0.1259(4)	3.911(3)
...							
f_m	0.014654	0.0150(4)	5.34(3)	0.0132(4)	5.38(3)	0.0094(4)	5.10(4)
$f_0 + f_m$	2.191442	0.0241(4)	3.45(2)	0.0168(4)	3.42(2)	0.0117(4)	3.45(3)
$2f_0 + f_m$	4.368230	0.0162(4)	1.42(3)	0.0142(4)	1.36(3)	0.0110(4)	1.40(3)
...							
$f_0 - f_m$	2.162134	0.0691(4)	4.896(6)	0.0546(3)	4.926(7)	0.0347(4)	5.02(1)
$2f_0 - f_m$	4.338922	0.0393(4)	1.46(1)	0.0313(4)	1.47(1)	0.0198(4)	1.45(2)
...							
$2f_0 + 2f_m$	4.382884	0.0010(4)	0.4(4)	0.0017(4)	1.4(2)	0.0024(4)	1.6(2)
$6f_0 + 2f_m$	13.09004	0.0013(4)	0.7(3)	0.0016(3)	5.8(2)	0.0008(4)	6.2(4)
...							
$f_0 - 2f_m$	2.147480	0.0028(4)	4.8(1)	0.0017(4)	4.1(2)	0.0015(4)	4.4(3)
$2f_0 - 2f_m$	4.324267	0.0058(4)	0.13(7)	0.0039(4)	0.10(9)	0.0025(4)	6.2(1)
...							
$6f_0 - 3f_m$	13.01676	0.0009(4)	5.9(4)	0.0010(3)	5.9(3)	0.0006(4)	6.1(6)
$f_1' = f_2' - f_0$	2.888023	0.0033(4)	3.9(1)	0.0024(4)	3.9(1)	0.0016(4)	4.2(2)
f_2'	5.064811	0.0016(4)	0.7(3)	0.0024(4)	1.4(2)	0.0023(4)	1.4(2)
$f_3' = f_2' + f_0$	7.241599	0.0028(4)	4.7(2)	0.0020(4)	4.8(2)	0.0016(4)	4.5(2)
$f_4' = f_2' + 2f_0$	9.418387	0.0017(4)	1.6(2)	0.0014(4)	1.6(2)	0.0015(4)	1.5(2)

these electronic data and give information regarding their form and content.

The times of the pulsation and Blazhko maxima (i.e. the zero pulsation and modulation phases) are determined from the light-curve solutions. The epoch of the pulsation corresponds to the time of the maximum of the mean pulsation light curve, which is constructed as a synthetic light curve using the Fourier components of the pulsation frequency and its harmonics of the full light-curve solution. The epoch of the modulation is defined as the time when the amplitude of the fundamental frequency is the highest. This epoch does not necessarily coincide with the time of the highest amplitude phase of the modulation. The elements are given in the following equations:

$$T_{\max}^{\mathrm{XY\,And}} = \mathrm{HJD}\,245\,4381.5513 + E_{\mathrm{puls}}^{\mathrm{XY\,And}} \times 0.3987247\,\mathrm{d}; \quad (1)$$

$$T_{\mathrm{Bl\,max}}^{\mathrm{XY\,And}} = \mathrm{HJD}\,245\,4379.9 + E_{\mathrm{mod}}^{\mathrm{XY\,And}} \times 41.37\,\mathrm{d}; \quad (2)$$

$$T_{\max}^{\mathrm{UZ\,Vir}} = \mathrm{HJD}\,245\,4470.2294 + E_{\mathrm{puls}}^{\mathrm{UZ\,Vir}} \times 0.4593925\,\mathrm{d}; \quad (3)$$

$$T_{\mathrm{Bl\,max}}^{\mathrm{UZ\,Vir}} = \mathrm{HJD}\,245\,4472.9 + E_{\mathrm{mod}}^{\mathrm{UZ\,Vir}} \times 68.24\,\mathrm{d}. \quad (4)$$

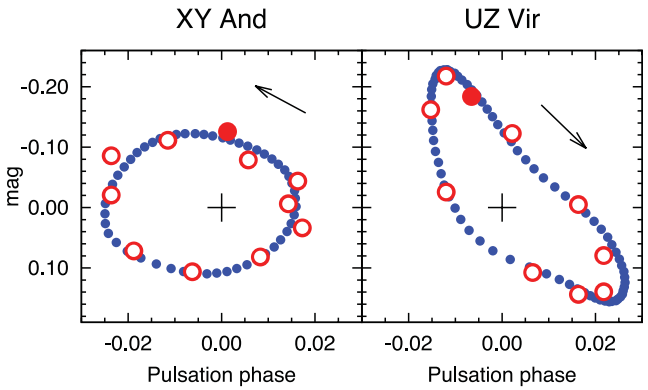

Figure 4. Brightness and phase variations of the pulsation-light maxima of XY And and UZ Vir in the V band. Large (red) circles mark the observations in 11 and 10 Blazhko phase bins. Filled circles represent the bins nearest to zero Blazhko phase, according to the elements given in equations (2) and (4). Small (blue) dots are generated from synthetic light-curve solutions using the frequencies given in Tables 5 and 6. Relative phases and magnitudes of the maxima with respect to the maximum of the mean pulsation light curve (marked by plus signs) are plotted. Arrows mark the directions of going around the loops; this is anticlockwise for XY And and clockwise for UZ Vir.

4 COMPARISON AND DETAILS OF THE MODULATION OF XY AND AND UZ VIR

As Fig. 1 shows, both the phase and the amplitude modulations of XY And are pronounced, while the fix point on the rising branch of the light curve of UZ Vir indicates that amplitude modulation is dominant in this star. The phase of the maximum brightness of both stars varies, however, within about the same ±0.02 pulsation-phase range in both stars, as can be seen in Fig. 4. This contradictory result means that the definition of the amplitude of the phase modulation is not at all straightforward.

The modulation of UZ Vir is of a rare type, because the amplitude of the low-frequency modulation components of the triplets are much larger than the high-frequency ones. The amplitude difference between the two modulation components of a triplet is characterized

by the asymmetry parameter, $Q = (A_+ - A_-)/(A_+ + A_-)$, introduced by Alcock et al. (2003). The results from both the MACHO project (Alcock et al. 2003) and the Konkoly Blazhko Surveys I and II (Sódor et al. 2012) show that the majority of Blazhko stars have a positive asymmetry parameter. The asymmetry parameter of UZ Vir, calculated for the triplet around f_0 in the V band, has an extremely large negative value: $Q = -0.53 \pm 0.01$. Among the 731 Blazhko RRab stars in the MACHO Large Magellanic Cloud (LMC) sample, only about 4 per cent have larger negative Q values (see fig. 10 of Alcock et al. 2003) than this value.

As Szeidl & Jurcsik (2009) have pointed out, a connection exists between the sign of the Q parameter and the travelling direction of the light maximum along the loop in the maximum phase–brightness plane. The negative Q parameter of UZ Vir reflects the property that its light maximum goes along the loop in a clockwise direction (see Fig. 4), while for most Blazhko stars either the maximum goes in the opposite, counterclockwise direction (as for XY And) or the loop is degenerate.

Examining Fig. 1, another significant difference between the modulation of the two Blazhko stars is discernible. The pulsation light curve of XY And is much smoother in each Blazhko phase than that of UZ Vir, especially around the light minimum. The bumps and humps, which characterize the light variation of UZ Vir, are completely missing from the light curve of XY And. This difference is also reflected in the light-curve solutions. Although the noise characteristics of the residual spectra of the two objects are similar, significantly more frequency components are needed for UZ Vir (i.e. 84), to describe its more complex brightness variation, than for XY And (i.e. 57). The harmonic components of the pulsation are detected up to $25f_0$ in UZ Vir, but only up to $13f_0$ in XY And. This also indicates that the mean pulsation light curve of XY And is more simple than that of UZ Vir.

4.1 Amplitude and phase relations of the pulsation light curve

Fig. 5 shows the amplitude versus phase variations of the first nine harmonic orders of the pulsation light curves of XY And and UZ Vir in 11 and 10 phase bins of their modulation cycles, respectively. The solid lines show the same loops derived from synthetic light-curve solutions. The directions of going around the curves are marked with arrows in the top-left panels. This direction remains the same for all the harmonic orders in both stars.

The phase–amplitude loops are dissimilar in the different harmonic orders for both stars, and none of the loops matches exactly the observed maximum phase–maximum brightness loops shown in Fig. 4. Furthermore, the maximum amplitude of the loops occurs in different Blazhko phases, as can be seen in Fig. 5, where the phases and amplitudes of the light curve at the zero Blazhko phase are denoted by solid symbols. Some of the highest-order loops show an interesting feature; they seem to 'open' at the lowest

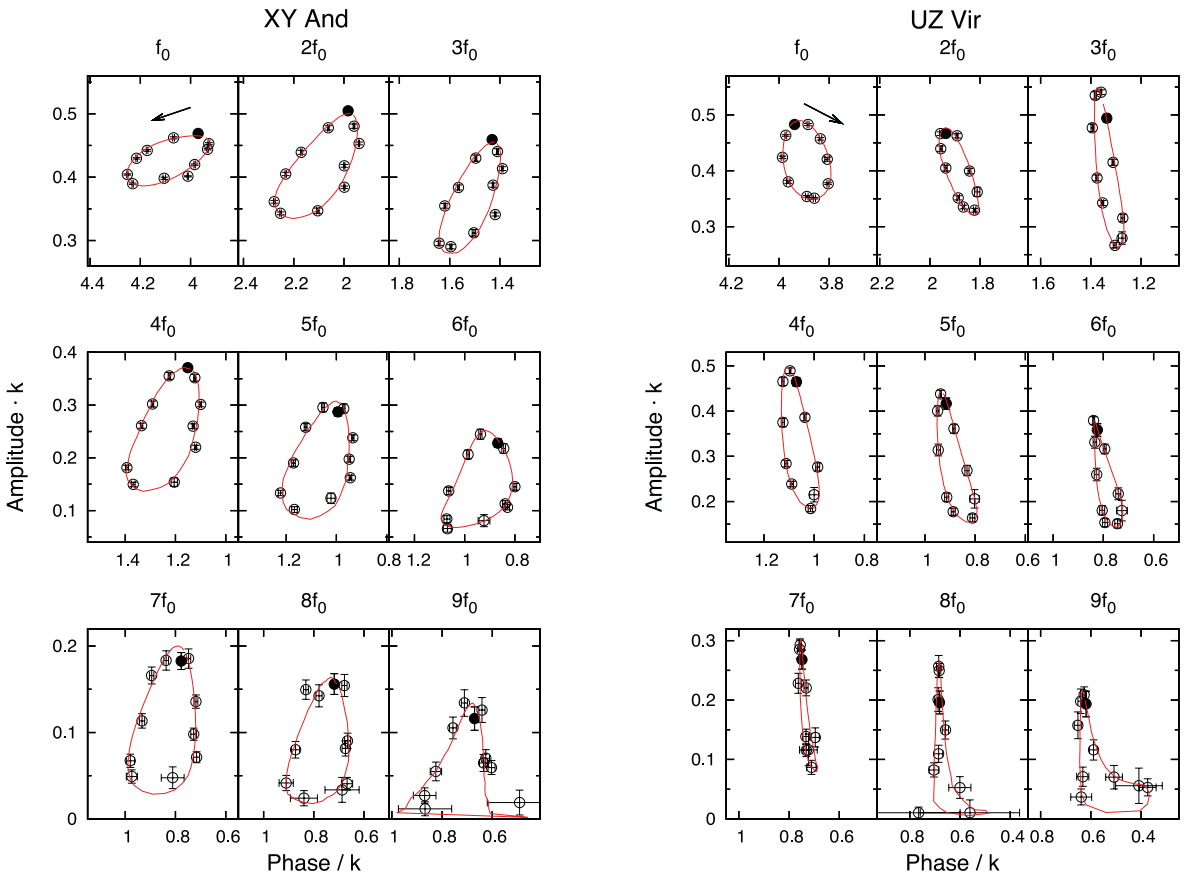

Figure 5. Amplitude versus phase variations (with uncertainties) of the first nine harmonic orders of the pulsation light curves of XY And and UZ Vir during their modulation cycles. Data of the bins nearest to the 0.0 Blazhko phase are marked with full dots. The solid lines show the same loops according to synthetic data. The amplitudes and phases are scaled by 'k', the harmonic order, for the better visibility. Note that the phase range is the same in each panel (i.e. 0.6 rad). The horizontal axes are reversed in order to be in accordance with the variation of the phase of the maxima shown in Fig. 4. The directions of going around the curves are marked with arrows in the top-left panels. This direction remains the same for all the harmonic orders in both stars.

amplitudes in the ninth and eighth–ninth orders for XY And and UZ Vir, respectively. In accordance with its more complex light variation, the phase–amplitude loops of UZ Vir show a large variety, from a circular shape (first order) to a quasi-degenerate shape (seventh order). However, with the exception of the ninth order, all the phase–amplitude loops of XY And are egg-shaped or elliptical.

4.2 Amplitude and phase relations of the triplet components

The relative amplitudes of the pulsation and modulation components,

$$R_k^+ = \frac{A_{kf_0+f_\mathrm{m}}}{A_{kf_0}}, \tag{5}$$

$$R_k^- = \frac{A_{kf_0-f_\mathrm{m}}}{A_{kf_0}}, \tag{6}$$

and the asymmetry parameter,

$$Q_k = \frac{A_{kf_0+f_\mathrm{m}} - A_{kf_0-f_\mathrm{m}}}{A_{kf_0+f_\mathrm{m}} + A_{kf_0-f_\mathrm{m}}}, \tag{7}$$

are derived for each harmonic order (k).

In order to follow the phase variations, we calculate the epoch-independent phase differences between the pulsation and the modulation components,

$$\chi_k^+ = \varphi_{kf_0+f_\mathrm{m}} - \varphi_{kf_0} - \varphi_{f_\mathrm{m}} \tag{8}$$

$$\chi_k^- = \varphi_{kf_0-f_\mathrm{m}} - \varphi_{kf_0} + \varphi_{f_\mathrm{m}} \tag{9}$$

and phase relations of the two modulation components,

$$\Phi_k = \varphi_{kf_0+f_\mathrm{m}} + \varphi_{kf_0-f_\mathrm{m}} - 2\varphi_{kf_0} \tag{10}$$

$$\Psi_k = \varphi_{kf_0+f_\mathrm{m}} - \varphi_{kf_0-f_\mathrm{m}} - 2\varphi_{f_\mathrm{m}}, \tag{11}$$

according to the Fourier solutions of the light curves given in Tables 5 and 6.

Fig. 6 shows the R_k^+, R_k^-, Q_k, χ_k^+, χ_k^-, Φ_k and Ψ_k amplitude and phase relations of the triplet components in the different harmonic orders for the observed bands of the two studied stars.

4.2.1 XY And

Both the amplitude and phase variations show smooth, gradual, almost monotonic changes. Fig. 6(a) (left) illustrates that while the low-frequency triplet components hardly change compared to the pulsation components, the amplitudes of the high-frequency components become as high as the amplitudes of the pulsation frequencies from the seventh harmonic order. As a result, the asymmetry parameter, Q_k, increases towards higher harmonic orders (Fig. 6b, left).

Figs 6(c) and (d) (left panels) display the phase-difference variations of the triplet components. Each of the four phase relations shows quite a regular behaviour. It is interesting to note that while we observe only a 0.5-rad gradual increase of the phase difference between the higher amplitude triplets and the pulsation components (χ_k^+), the phase difference of the lower amplitude triplet component (χ_k^-) is less stable and it changes within about 1.5 rad. The Φ_k and Ψ_k phase relations also show monotonic changes with increasing gradients towards higher harmonic orders.

The most interesting feature of the phase relations is that each of the four shows a definite colour dependence, which is most pronounced for χ_k^- and Ψ_k. These phase relations in the V and I_C bands differ systematically in each harmonic order by 0.3–1.0 rad. The Q_k asymmetry parameter might also be somewhat colour-dependent; the asymmetry of the triplets seems to be slightly larger in the I_C band than in the V band. However, this tendency is not really significant.

4.2.2 UZ Vir

The amplitude and phase relations of the triplets of UZ Vir (the right-hand panels of Fig. 6) show a more complex behaviour than for XY And. Most probably, this is the consequence of the appearance and disappearance of the bump/hump features on the light curve during the modulation cycle.

The amplitude variation of the lower amplitude triplet component, R_k^+, is smoother than that of the higher amplitude triplet component, R_k^-, which shows local maxima at the fifth and ninth–tenth orders. The variation of the asymmetry parameter is also complex. It has local minima (taking into account the negative values of Q_k, these correspond to large asymmetry) in the first, fourth–fifth and ninth–tenth harmonic orders. Towards higher orders, the asymmetry of the triplets ($|Q_k|$) shows a decreasing tendency, while it increases for XY And.

The phase behaviour of the triplet components of UZ Vir is not smooth either. The total range of the variations of χ_k^+, χ_k^- and Φ_k is 1.5–2 rad, while the variation of Ψ_k extends to 2.5 rad. The χ_k^- phase difference follows a similar change to the variations of the asymmetry parameter with local minima in the third and eighth orders. With the exception of the first order of Φ_k, the variations of Ψ_k and Φ_k reflect the changes of χ_k^+ and χ_k^-, respectively.

A colour dependence of the phase relations of UZ Vir is also detected. The χ_k^+ and Ψ_k values are systematically larger by 0.1–0.5 rad in the I_C band than in the B and V bands, while the colour dependence seen in the χ_k^- data is the opposite. With the exception of the first order, the asymmetry parameter of UZ Vir is also colour-dependent. In contrast to the results for XY And, the triplets are less asymmetric towards longer wavelengths here.

5 PHYSICAL PARAMETERS AND THEIR VARIATION DURING THE MODULATION

The variations of the pulsation-averaged atmospheric parameters of XY And and UZ Vir during the Blazhko cycle are derived using the Baade–Wesselink IPM (Sódor, Jurcsik & Szeidl 2009). These parameters are the effective temperature (T_eff), luminosity (L), radius (R) and effective surface gravity ($\log g$). Utilizing multicolour light curves and synthetic colours from static atmosphere models (Castelli & Kurucz 2003), the method can be used to find the best-fitting model parameters through the variation of template T_eff and V_rad curves. In order to test the stability and reliability of the method, different V_rad template curves and different weightings are applied. Therefore, similarly to the previous analyses, the IPM code is run with four different internal settings (for details, see Sódor et al. 2009, table 1) to estimate the inherent, method-specific uncertainty of the results.

5.1 Constant parameters

To apply the IPM, the Blazhko-phase-independent parameters have to be known first. These are the metallicity ([Fe/H]), mass (M), distance (d) and the mean dereddened colours of the variables averaged over both the pulsation and modulation periods.

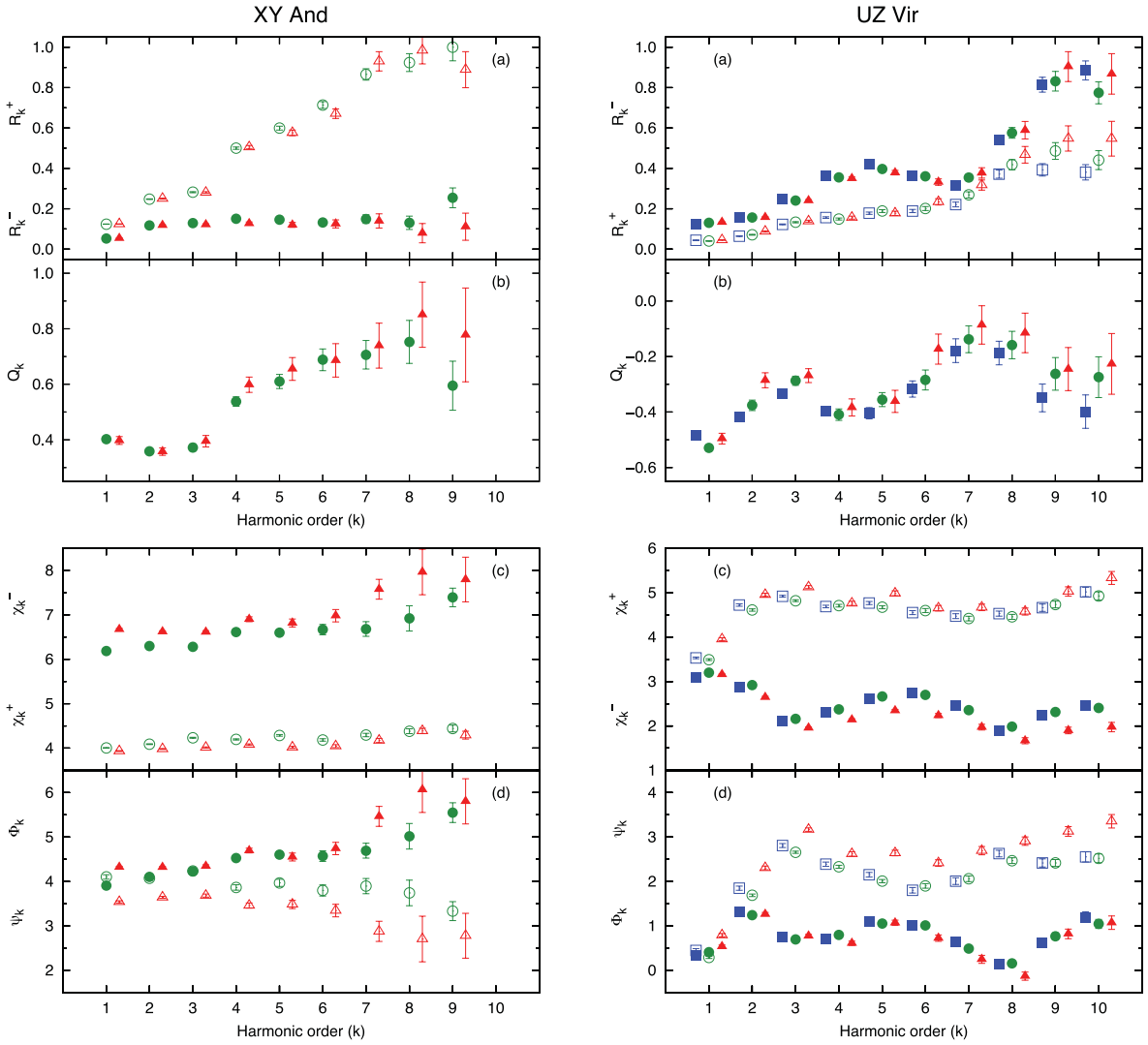

Figure 6. Amplitude and phase relations of the triplet components of XY And and UZ Vir in the different harmonic orders. Squares (blue), circles (green) and triangles (red) denote the results in the B, V and I_C bands, respectively. Results for the different photometric bands of the same harmonic order are shifted horizontally for better visibility. (a) $R_k^+ = A_{kf_0+f_m}/A_{kf_0}$ (empty) and $R_k^- = A_{kf_0-f_m}/A_{kf_0}$ (filled) amplitude ratios of the triplet components relative to the harmonic components of the pulsation. (b) $Q_k = (A_{kf_0+f_m} - A_{kf_0-f_m})/(A_{kf_0+f_m} + A_{kf_0-f_m})$, the asymmetry parameter. (c) $\chi_k^+ = \varphi_{kf_0+f_m} - \varphi_{kf_0} - \varphi_{f_m}$ (empty) and $\chi_k^- = \varphi_{kf_0-f_m} - \varphi_{kf_0} + \varphi_{f_m}$ (filled), the phase differences between the modulation components and the harmonics of the pulsation. (d) $\Phi_k = \varphi_{kf_0+f_m} + \varphi_{kf_0-f_m} - 2\varphi_{kf_0}$ (filled) and $\Psi_k = \varphi_{kf_0+f_m} - \varphi_{kf_0-f_m} - 2\varphi_{f_m}$ (empty) phase relations of the pulsation and the modulation components.

The metallicity of XY And was measured by spectroscopic (Layden 1994) and photometric (Jurcsik & Kovács 1996) means. Both methods yield the same result, −0.68 dex (Jurcsik et al. 2009, table 5). Therefore, as a reliable estimate for the metallicity of XY And, this value is accepted and applied throughout the following analysis. No spectroscopic measurement of the metallicity of UZ Vir has been published. Jurcsik et al. (2009) have shown that a well-defined mean pulsation light curve of a Blazhko star yields a reliable metallicity value, according to the [Fe/H](P, Φ_{31}) formula (Jurcsik & Kovács 1996), even for strongly modulated RR Lyrae stars. This method gives [Fe/H] = −0.90 dex for UZ Vir. However, the example of RZ Lyr means that, in certain cases, the photometric metallicity can differ by as much as ∼0.4 dex from the spectroscopic value (Jurcsik et al. 2012). Therefore, the effect of the choice of the input metallicity on the IPM results is also checked by calculating the mean physical parameters of UZ Vir using two other metallicity values. Because only the evolutionary possible values of the mean physical parameters are accepted, the other metallicity values (−0.65 and −1.26) were selected from the [Fe/H] values of the horizontal branch evolutionary models of Dorman (1992).

Our differential photometric observations do not allow us to determine the mean (reddened) colours of these two variables, because no standard multicolour magnitude measurement of the comparison stars, or of any other object in the field of view, is available. Schmidt & Seth (1996) have given intensity-averaged values of $(V) - (R) = 0.22 \pm 0.02$ and 0.24 ± 0.03 mag for XY And and UZ Vir, respectively. However, these colour indices should be treated with caution, because they are calculated from only 10–20 data points per band, observed in different Blazhko phases. Therefore, the uncertainties of these colours are estimated to be a few hundredths magnitude higher than the values given by Schmidt & Seth (1996). According to the extinction maps of Schlegel, Finkbeiner & Davis (1998), the interstellar reddening $E(B - V)$ towards the directions of XY And and UZ Vir is 0.050 and 0.026 mag, respectively. Because these

Table 7. Mean physical parameters and their uncertainties derived from the mean pulsation light curves of XY And and UZ Vir with the IPM using static atmosphere models with different [Fe/H] metallicities. The luminosities, temperatures and masses are constrained to match the evolutionary possible values for horizontal-branch stars. The mean physical parameters are also required to fit the pulsation period via the pulsation equation. (M_V) denotes the intensity-averaged absolute V magnitude.

Object	[Fe/H] (dex)	M ($M_\odot$)	d (pc)	(M_V) (mag)	R ($R_\odot$)	L ($L_\odot$)	$T_{\rm eff}$ (K)
XY And	−0.68	0.58 ± 0.01	3700 ± 200	0.76 ± 0.05	4.15 ± 0.20	40.5 ± 2.5	7100 ± 100
UZ Vir	−0.65	0.61 ± 0.01	2850 ± 150	0.77 ± 0.05	4.54 ± 0.20	41.0 ± 2.5	6800 ± 100
UZ Vir	−0.90	0.59 ± 0.01	2900 ± 150	0.71 ± 0.05	4.55 ± 0.20	43.5 ± 2.5	6900 ± 100
UZ Vir	−1.26	0.57 ± 0.01	2950 ± 150	0.65 ± 0.05	4.56 ± 0.20	46.0 ± 2.5	7000 ± 100

values also have uncertainties of the order of 0.01 mag, and because these are only upper limits for the actual reddenings, the possible colour ranges, and consequently the possible overall temperature ranges, are too wide to impose any meaningful constraint on the IPM fitting process.

Therefore, the temperature, luminosity and mass of both stars have been constrained using the results of the pulsation equation and horizontal branch (HB) evolutionary model. According to the pulsation equation of Marconi et al. (2003, equation 1a) and the HB evolutionary models of Dorman (1992, figs 7–10), the pulsation periods of the studied objects correspond to the following physical parameter ranges: temperature of 7000–7200 and 6700–7100 K and luminosity of 38–43 and 38.5–48.5 $L_\odot$ for XY And and UZ Vir, respectively.

Applying these constraints, the IPM is run for the mean pulsation light curves of both objects to determine consistent sets of mean and constant parameters. The results from these runs are listed in Table 7. To check the effect of the uncertainty in the metallicity of UZ Vir, the mean physical parameters are calculated for three possible metallicity values. The distances are estimated by accepting $\langle V \rangle = 13.73$ and 13.05 mag (Schmidt & Seth 1996) and assuming $A(V) = 3.14E(B-V) = 0.157$ and 0.082 interstellar absorption for XY And and UZ Vir, respectively. The uncertainties given in Table 7 are estimated by taking into account the inherent error of the method, the uncertainties of the input parameters and the possible ranges of the constrained parameters, according to the HB evolutionary models of Dorman (1992). The data given in Table 7 prove that the three possible metallicity values of UZ Vir result in similar uncertainties of the output parameters as the other factors together. The only exception is the radius, which is practically the same for all three input metallicities.

5.2 Blazhko-phase-dependent parameters

Fixing the Blazhko-phase-independent physical parameters to their values determined in Section 5.1 and listed in Table 7, the IPM is run using the light curves of XY And and UZ Vir in 11 and 10 different, disjunct phase bins of the modulation, respectively. In order to obtain the highest possible number of Blazhko phase bins with full pulsation-phase coverage, the bins are not exactly equidistant, but are spread over the Blazhko cycle almost evenly. Each bin is narrow enough for the pulsation light curves not to be affected by Blazhko-phase smearing.

The IPM is run for UZ Vir with the three possible metallicities listed in Table 7 to check its effect on the results. It is found that the different metallicity values affect only the means of the physical parameters, but the amplitudes and the phase relations of their variations with the Blazhko phase remains practically the same. Therefore, only the results obtained with the most likely value of [Fe/H] = −0.90 dex are shown.

The IPM gives the radius, luminosity, temperature and surface-gravity changes during the pulsation in each phase bin of the modulation. The pulsation-averaged mean values of these quantities characterize the global mean changes in the stellar parameters during the modulation cycle. Similarly to the IPM results of the previous investigations of Blazhko stars, the actual values of the fixed or constrained physical parameters influence the averages of the other physical parameters. Nevertheless, they affect the variations during the Blazhko cycle only slightly. The amplitudes of the solutions differ somewhat if the input parameters are varied within their possible ranges (Table 7), but the relative sign of their variations remains unchanged.

The appearance of $f_{\rm m}$ in the frequency solution of the light curves reflects the variation of magnitude-averaged mean brightness in the different bands during the modulation. The IPM, which also utilizes colour information, discloses what luminosity, radius and temperature changes are required to describe the observed changes in the mean magnitudes. The IPM results on XY And and UZ Vir are plotted against the modulation phase in Fig. 7. Here, we plot the observed (left-hand panels) and IPM-derived (right-hand panels) variations of the pulsation-averaged parameters during the Blazhko modulation. The observed parameters (from top to bottom) are the amplitude of the main pulsation frequency (f_0), the Φ_1 phase variation of this frequency component, and the pulsation-period variations deduced from the observed phase variations of the f_0 component, and the different averages of the light and colour curves according to magnitude- and intensity-scale representations.

6 DISCUSSION AND SUMMARY

6.1 Light-curve modulation

The Fourier spectra of the light curves of XY And and UZ Vir are described by multiplet frequencies ($kf_0 \pm nf_{\rm m}$) and the modulation frequency ($f_{\rm m}$), typical of Blazhko stars. The multiplet structures are triplets and quintuplets, with a single septuplet component in the spectrum of UZ Vir ($6f_0 - 3f_{\rm m}$). The phase of the rising branch of XY And is strongly modulated, while a fix point on the rising branch of UZ Vir (see Fig. 1) indicates that amplitude modulation dominates its light-curve variation. Looking at the phase variations of the maximum brightness of the two stars, similar amplitude changes are observed, as shown in Fig. 4. This controversial behaviour of the phase variations of the rising branches and the maxima means that the strength of the phase modulation at different parts of the pulsation light curve can be rather different.

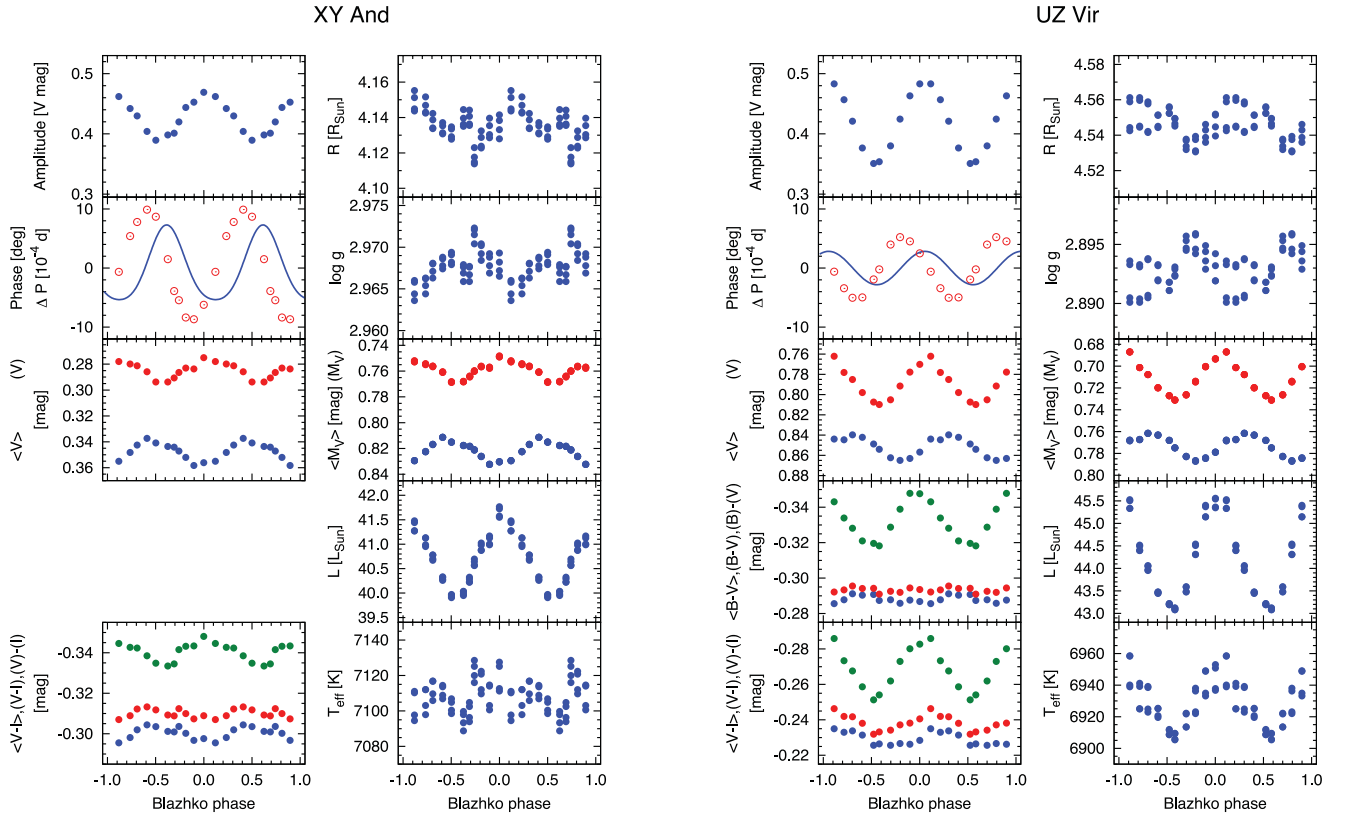

Figure 7. The mean observed (left-hand panels) and the IPM-derived physical parameters (right-hand panels) of XY And and UZ Vir in different phases of the modulation. From top to bottom, the left-hand panels show: amplitude modulation – amplitude of the f_0 frequency component; pulsation-phase or period modulation – variation of the phase of the f_0 pulsation component (empty circles) and deviation of the instantaneous pulsation period from the mean pulsation period (continuous line); pulsation-averaged V magnitude; pulsation-averaged $B - V$ colour; pulsation-averaged $V - I_C$ colour. Magnitude- and intensity-averaged brightnesses and colours are denoted by angle and round brackets, respectively. From top to bottom, the right-hand panels show the pulsation averages of the following physical parameters: radius, surface gravity, absolute visual magnitude, luminosity and effective temperature. The results of four different settings of the IPM are shown in order to indicate the inherent uncertainty of the method.

The pulsation light curve of XY And is much smoother in each Blazhko phase than that of UZ Vir. Consequently, the light-curve solution of XY And involves fewer pulsation and modulation components than that of UZ Vir.

The modulation of UZ Vir is of a rare type, because the amplitude of the low-frequency triplet components is significantly larger than that of the high-frequency ones. Accordingly, the light maximum goes in a clockwise direction around the loop on the pulsation phase–brightness plane (Fig. 4). However, for most Blazhko stars, either the maximum goes around in the opposite direction, or the loop is degenerate.

For the first time, the amplitude and phase relations of the triplet components are also studied in detail. No common feature of the variations of the defined parameters of the two stars has been recognized. This result supports the fact that Blazhko stars behave very individually. It is difficult, if at all possible, to find any overall, common property of the modulation. The most interesting finding of this investigation is the detection of the colour dependency of the asymmetry parameter and the phase relations. The colour dependence of these quantities is the opposite for each of the two stars, which might be connected to the fact that their amplitude and phase variations have opposite signs during the Blazhko cycle. The colour dependence of the amplitude and phase relations of the triplets of other Blazhko stars should be studied in order to decide whether such a connection really holds. Because the detected colour dependence carries important physical information about the modulation, a further investigation and explanation of this should be an important step in the description and interpretation of the Blazhko effect.

6.2 Additional frequencies

The additional frequencies in RR Lyrae stars have been discovered only recently, because very precise and extended photometry is needed to find these low-amplitude signals.

Both XY And and UZ Vir show variability besides the pulsation and modulation with an additional, independent frequency. A series of four peaks appears in the Fourier spectra of both objects with a separation that equals their pulsation frequency. One of these peaks is identified as a linearly independent frequency component, while the other three members of the series are interpreted as linear combinations of this and the pulsation frequency. The frequency ratios of the possible main components of the additional frequency series (f_0/f) are 0.325 for XY And and 0.754, 0.430 or 0.301 for UZ Vir. The 0.301, 0.325 and 0.430 frequency ratio values cover the possible regime of the third–sixth radial overtones. Unfortunately, the actual frequencies of the higher-order radial modes on a large grid of stellar parameters have never been published. Thus, we do not know whether or not the observed frequency ratios fit any higher-order radial mode. However, because RR Lyrae models indicate that these higher-order modes are strongly damped, we consider it unlikely that radial modes have been detected in these stars.

In the case of XY And, two possible explanations of the additional frequency series have been raised: (i) one frequency of the

series might be a non-radial mode; (ii) all four frequencies correspond to a secondary modulation of an extremely short period, ∼5.01 d. To explain the series of additional frequencies in UZ Vir, we have also raised two possibilities: (i) the frequency at 2.89 c d^{-1} might be the first radial overtone, but with an unusually large f_0/f_1 ratio of 0.754; (ii) one of the two highest amplitude components of the additional frequency series corresponds to a non-radial mode. The recent detection of an additional frequency with a 0.753–758 frequency ratio in the *Kepler* data of RR Lyrae (Molnár et al. 2012), which has been identified with the first overtone mode, also favours the first possibility in the case of UZ Vir.

It is interesting to examine the reported occurrences of other additional frequencies among RR Lyrae variables. Both double-mode RR Lyrae stars with extended satellite observations (AQ Leo and *CoRoT* ID 0101368812; Gruberbauer et al. 2007; Chadid 2012) show additional frequencies beyond the fundamental and the first overtone modes. Many Blazhko variables have one or more extra independent frequencies in their light variation, in addition to the pulsation and modulation components. Such frequencies have been reported by Chadid et al. (2010), Poretti et al. (2010) and Guggenberger et al. (2011, 2012); see also table 2 of Benkő et al. (2010). The $\pm 12.5 f_m$ peaks around some of the pulsation components in MW Lyr (Jurcsik et al. 2008a) might also be connected to an additional frequency, as suggested by Poretti et al. (2010). In contrast, only two of the 19 non-modulated RRab stars observed by *Kepler* show frequencies besides the fundamental-mode pulsation (Nemec et al. 2011), and no additional frequency has been detected in the only non-Blazhko *CoRoT* RRab star analysed so far (Paparó et al. 2009). Also, no additional frequency has been found in the residual spectra of the 14 non-modulated RRab stars observed in the Konkoly Blazhko Survey I (see references in Jurcsik et al. 2009). Although the majority of the *Kepler* Blazhko targets have not yet been analysed thoroughly, it is clear that the occurrence rate of the appearance of additional frequencies is much higher among modulated RRab stars than for non-modulated RRab stars. A possible explanation might be that the changing physical parameters during the Blazhko cycle (Jurcsik et al. 2008b) temporarily fulfil the conditions required for the excitation of the other observed (radial or non-radial) modes, whereas the chance to satisfy the excitation conditions is much smaller for the RRab stars that have stable light curves. A similar explanation has been suggested for the appearance of a peculiar bump on the descending branch of RZ Lyr in the low-amplitude phases of its modulation (Jurcsik et al. 2012). However, the excited additional mode of RZ Lyr is supposed to be in resonance with one of the harmonics of the main pulsation frequency, which explains why it does not appear in the Fourier spectrum as an additional frequency directly.

6.3 Physical parameter changes during the modulation

The modulational changes in the atmospheric parameters of XY And and UZ Vir have been derived by applying the IPM. Unlike the many differences between the Blazhko modulation properties of the two objects, their mean physical parameters are rather similar; XY And is only ∼150 K hotter, ∼4 $L_\odot$ fainter, ∼0.4 $R_\odot$ smaller, ∼0.01 $M_\odot$ less massive and ∼0.22 dex more metal-rich than UZ Vir. The changes in the mean temperature, radius and luminosity during the Blazhko cycle of the two stars also do not show any significant difference.

Both objects show a strong luminosity variation during the modulation: $\Delta L \approx 2$ and ≈ 2.5 $L_\odot$ are derived for XY And and UZ Vir, respectively. Similar to all Blazhko RR Lyrae stars analysed with the IPM so far, XY And and UZ Vir are brightest when the pulsation amplitude is highest.

The radius variation is weak; the average radius is highest around the Blazhko maximum in both variables. The IPM results show only marginal temperature variation of XY And during the Blazhko cycle, but the $T_{\rm eff}$ and (V)–(I_C) curves together suggest that XY And is about 10–20 K warmer at the high-amplitude phase of the modulation than when the pulsation amplitude is lowest. The IPM results for UZ Vir indicate only a modest but definite modulational variation of about 30 K in temperature. Both the radius and temperature are highest at the Blazhko maximum for both XY And and UZ Vir.

The Blazhko model proposed by Stothers (2006) postulates a changing magnetic field in the envelope of the star, which influences the parameters of convection. The model makes predictions about the phase relation between the amplitude and period modulations and between the period modulation and radius variation (Stothers 2011); that is, these relations depend on the temperature of the star. For hot RRab stars, the model of Stothers (2006) predicts that the pulsation period is decreasing at the high-amplitude Blazhko phase (the period and amplitude variations are in anti-phase), while for stars below the crossover temperature of about 6400 K, the period is increasing at the same Blazhko phase (the changes of the two quantities are in phase). These relations are shown in the top two panels in the left columns of Fig. 7 for the two studied objects (the changes in the pulsation period are plotted with the solid line). The two variables have similar temperatures, well above the predicted crossover value, and they also have similar pulsation periods and metallicities. Still, the phase relations between their pulsation amplitude and pulsation period variation are the opposite of each other. This behaviour is also demonstrated in Fig. 4, which shows that the maxima of the two objects go along their modulational loops in the pulsation phase–brightness plane in opposite directions.

The Stothers model also expects a relation between the pulsation period and radius variation during the Blazhko cycle (Stothers 2011). The model predicts anticorrelated variation between these two quantities in hot RRab stars, which turns into a correlation for cooler RRab variables. However, both objects are hot, short-period RRab stars, and both have the highest radius at the Blazhko maximum, while their variations in pulsation period are the opposite of each other.

These findings do not agree with the predictions of the Stothers model (Stothers 2006, 2011), which claims that two Blazhko stars with such similar properties are expected to display similar relations between their amplitude, pulsation period and radius variations. Our results show that even if the fundamental idea of the Stothers model is right, the relations between the studied properties of the Blazhko stars are more complicated than are predicted by the model in its present form.

ACKNOWLEDGMENTS

The support of Hungarian Scientific Research Fund (OTKA) grants K-076816 and K-081373 is acknowledged.

REFERENCES

Alcock C. et al., 2003, ApJ, 598, 597
Benkő J. M. et al., 2010, MNRAS, 409, 1585
Buchler R., Kolláth Z., 2001, ApJ, 555, 961
Buchler R., Kolláth Z., 2012, ApJ, 731, 24

Castelli F., Kurucz R. L., 2003, in Piskunov N., Weiss W. W., Gray D. F., eds, Proc. IAU Symp. 210, Modelling of Stellar Atmospheres. Astron. Soc. Pac., San Francisco, p. A20
Chadid M., 2012, A&A, 540, 68
Chadid M. et al., 2010, A&A, 510, 39
Deeming T. J., 1975, Ap&SS, 36, 137
Dorman B., 1992, ApJS, 81, 221
Dziembowski W., Cassisi S., 1999, Acta Astron., 49, 371
Gruberbauer M. et al., 2007, MNRAS, 379, 1498
Guggenberger E., Kolenberg K., Chapellier E., Poretti E., Szabó R., Benkő J. M., Paparó M., 2011, MNRAS, 415, 1577
Guggenberger E. et al., 2012, MNRAS, 424, 649
Jurcsik J., Kovács G., 1996, A&A, 312, 111
Jurcsik J. et al., 2008a, MNRAS, 391, 164
Jurcsik J. et al., 2008b, MNRAS, 393, 1553
Jurcsik J. et al., 2009, MNRAS, 400, 1006
Jurcsik J. et al., 2012, MNRAS, 423, 993
Kolláth Z., 1990, Occ. Techn. Notes Konkoly Obs., No. 1, http://www.konkoly.hu/staff/kollath/mufran.html
Kolláth Z., Molnár L., Szabó R., 2011, MNRAS, 414, 1111
Kovács G., 2009, in Guzik J. A., Bradley P., eds, AIP Conf. Proc. 1170, Stellar Pulsation: Challenges for Theory and Observation. Am. Inst. Phys., New York, p. 261
Layden A., 1994, AJ, 108, 1016
Marconi M., Caputo F., Di Criscienzo M., Castellani M., 2003, ApJ, 596, 299
Molnár L., Kolláth Z., Szabó R., 2012, MNRAS, 424, 31
Molnár L., Kolláth Z., Szabó R., Bryson S., Kolenberg K., Mullally F., Thompson S. E., 2012, ApJL, 757, 13
Nemec J. M. et al., 2011, MNRAS, 417, 1022
Paparó M., Szabó R., Benkő J. M., Chadid M., Poretti E., Kolenberg K., Guggenberger E., Chapellier E., 2009, in Guzik J. A., Bradley P., eds, AIP Conf. Proc. 1170, Stellar Pulsation: Challenges for Theory and Observation. Am. Inst. Phys., New York, p. 240
Poretti E. et al., 2010, A&A, 520, 108
Schlegel D. J., Finkbeiner D. P., Davis M., 1998, ApJ, 500, 525
Schmidt E. G., Seth A., 1996, AJ, 112, 2769
Smolec R., Moskalik P., Kolenberg K., Bryson S., Cote M. T., Morris R. L., 2011, MNRAS, 414, 2950
Sódor Á., 2012, Occ. Techn. Notes Konkoly Obs., No. 15, http://konkoly.hu/staff/sodor/lcfit.html
Sódor Á., Jurcsik J., Szeidl B., 2009, MNRAS, 394, 261
Sódor Á. et al., 2012, in Shibahashi H., ed., ASP Conf. Ser. Vol. 462, Progress in Solar/Stellar Physics with Helio- and Asteroseismology. Astron. Soc. Pac., San Francisco, p. 228
Stothers R. B., 2006, ApJ, 652, 643
Stothers R. B., 2011, PASP, 123, 127
Szeidl B., Jurcsik J., 2009, Commun. Asteroseis., 160, 17

APPENDIX A: SAMPLES OF THE ELECTRONIC TABLES

The full tables, containing the observations of UZ Vir and XY And (Tables A1–A5), are available as Supporting Information with the online version of this paper.

Table A1. CCD ΔV observations and derived colour indices of XY And, relative to the comparison star 2MASS 01270016+3404307.

HJD − 240 0000	ΔV (mag)	$\Delta V - I$ (mag)
54390.46709	0.466	−0.211
54390.47001	0.483	−0.201
...	...	...

Table A2. CCD ΔI_C time series of XY And.

HJD − 240 0000	ΔI_C (mag)
54390.46855	0.677
54390.47148	0.678
...	...

Table A3. CCD ΔV observations and derived colour indices of UZ Vir, relative to the comparison star 2MASS 13082756+1322403.

HJD − 240 0000	ΔV (mag)	$\Delta B - V$ (mag)	$\Delta V - I$ (mag)
54504.57397	1.183	−0.210	−0.109
54504.57976	1.191	−0.217	−0.102
...	...	...	...

Table A4. CCD ΔB time series of UZ Vir.

HJD − 240 0000	ΔB(mag)
54504.57158	0.975
54504.57737	0.986
...	...

Table A5. CCD ΔI_C time series of UZ Vir.

HJD − 240 0000	ΔI_C(mag)
54504.57515	1.309
54504.58108	1.296
...	...

SUPPORTING INFORMATION

Additional Supporting Information may be found in the online version of this article.

Table 5. Frequencies, amplitudes and phases of the V and I_C light-curve solutions (epoch = 54390.0, sine decomposition) of XY And.
Table 6. Frequencies, amplitudes and phases of the B, V and I_C light-curve solutions (epoch = 54404.0, sine decomposition) of UZ Vir.
Table A1. CCD ΔV observations and derived colour indices of XY And, relative to the comparison star 2MASS 01270016+3404307.
Table A2. CCD ΔI_C time series of XY And.
Table A3. CCD ΔV observations and derived colour indices of UZ Vir, relative to the comparison star 2MASS 13082756+1322403.
Table A4. CCD ΔB time series of UZ Vir.
Table A5. CCD ΔI_C time series of UZ Vir.

Please note: Wiley-Blackwell are not responsible for the content or functionality of any supporting materials supplied by the authors. Any queries (other than missing material) should be directed to the corresponding author for the article.

This paper has been typeset from a TEX/LATEX file prepared by the author.